Iranian Journal of Numerical Analysis and Optimization
Vol. ??, No. ??, ??, pp ??
https://doi.org/??
https://ijnao.um.ac.ir/

CC BY NC

Research Article

An appropriate fractional Narayana polynomials neural network method for dental caries infection model

H. Hassani*, Z. Avazzadeh, A. Turan-Dincel and H. Farahmand

Abstract

Dental caries represents a major global health challenge, affecting individuals of all ages and from various socioeconomic backgrounds. Despite advancements in preventive measures and treatments, it remains the most prevalent chronic disease worldwide, severely impacting both oral and overall health. This condition arises from complex interactions between microorganisms, the host's biological makeup, diet, environmental factors, and behavioral patterns. These

*Corresponding author

Received ??? ; revised ??? ; accepted ???

Hossein Hassani
Department of Mathematics, Anand International College of Engineering, Jaipur 303012, India. e-mail: hosseinhassani40@yahoo.com

Zakieh Avazzadeh
Stony Brook Institute at Anhui University, Anhui University, Hefei 230601, China. e-mail: z.avazzadeh@ahu.edu.cn

Arzu Turan-Dincel
Department of Mathematical Engineering, Yildiz Technical University, 34220, Esenler, Istanbul-Turkey. e-mail: artur@yildiz.edu.tr

Hanieh Farahmand
Department of Oral and Maxillofacial Medicine, School of Dentistry, Yasuj University of Medical Sciences, Yasuj, Iran. e-mail: haneyeh.farahmand@yums.ac.ir

How to cite this article
Hassani, H., Avazzadeh, Z., Turan-Dincel, A. and Farahmand, H., An appropriate fractional Narayana polynomials neural network method for dental caries infection model. *Iran. J. Numer. Anal. Optim.*, ??; ??(??): ??-??. ??

factors collectively contribute to the gradual demineralization and breakdown of tooth structures, leading to cavities and tooth decay. To address the mathematical model for simulating the spread of dental caries, a more accurate and effective neural network-based optimization (NNO) technique is suggested. In the present contribution, we introduce new fractional Narayana polynomials (FNPs). The NNO method consists of three main layers, which include an input layer, a hidden layer, and an output layer. The time variable (in months) is employed as an input parameter to the NNO method. Within the structure of the neural network, FNPs are employed as activation functions in the hidden layer, whereas the $arcsinh(t)$ function is utilized for the output layer. The mathematical model for dental caries is reduced to the problem of solving a system of algebraic equations through the use of FNPs, NNO and the Lagrange multiplier method. The convergence analysis, existence and uniqueness of solutions are discussed. The validity of the proposed NNO method is confirmed through relevant simulations. With its high efficiency and accuracy, the proposed NNO method proves to be an effective tool for analyzing the mathematical model for dental caries, showing significant potential for applications in two-dimensional differential equations and optimal control problems.

AMS subject classifications (2020): 41A10; 65Z05; 92C42.

Keywords: Fractional Narayana polynomials neural network; Dental caries infection model; Optimization algorithm; Lagrange multiplier method.

1 Introduction

The development of dental caries is driven by an imbalance between the demineralization and remineralization processes in the enamel. Acid-producing bacteria within plaque biofilm metabolize fermentable carbohydrates such as glucose, sucrose, and fructose into acids that erode the enamel and dentin, initiating caries formation [10]. As a result, dental caries is considered a microbial dietary disease, requiring both a cariogenic biofilm and frequent exposure to fermentable sugars [18, 43]. This continuous interaction between diet and microorganisms plays a crucial role in the progression of the disease [24]. Host susceptibility significantly influences the onset and progression of dental caries. Genetic factors affect immune responses, enamel structure, and saliva production, all of which impact an individual's resistance to cariogenic bacteria [35]. Salivary properties including pH, buffering capacity, and antimicrobial components help neutralize acids and regulate bacterial growth [25]. Additionally, fluoride exposure strengthens enamel and inhibits bacterial metabolism, making it a key factor in caries prevention. However, disparities in access to fluoridated water and dental products contribute to variations in caries prevalence across different populations [37]. Beyond biological and dietary influences, environmental and

behavioral factors also increase the risk of dental caries. Socioeconomic status affects access to dental care, oral health education, and fluoride-based products [41]. Poor oral hygiene promotes bacterial biofilm accumulation, leading to prolonged acid exposure and accelerated enamel demineralization, thereby increasing the risk of caries [36]. Furthermore, frequent consumption of fermentable carbohydrates creates an acidic oral environment, promoting both enamel breakdown and bacterial biofilm formation [27]. Several key risk factors contribute to dental caries: a history of caries, plaque accumulation, inadequate fluoride exposure, diet, reduced salivary flow, and poor overall health status [12]. Untreated dental caries in permanent teeth remains a widespread health issue, emphasizing the urgent need for improved prevention strategies and early interventions [17].

In recent years, mathematical models have emerged as a powerful tool for representing complex biological systems. A large number of numerical and neural network (NN) methods have been carried out in practical fields such as mathematical models of diverse diseases. Li and Yang [22] applied a numerical method based on the linearly implicit Euler method for an HIV model with latently infected T cells. Wang et al. [42] discussed the numerical solution of an HIV model by employing the linearly implicit Euler method with a general transmission dynamic. He [14] proposed a machine learning technique to obtain the solution of the HIV model of CD4(+). Sabir, Ben Said, and Al-Mdallal [33] investigated the numerical performances of the fractional-order mathematical influenza disease model by designing the computational framework based on the stochastic Levenberg–Marquardt backpropagation NNs. Moreover, Sabir et al. [32] presented the numerical solutions of the chickenpox disease model by applying a proficient optimization framework based on the artificial NN. Anusha Bamini et al. [3] used the convolutional NN in deep learning technique for premature detection of Alzheimer's disease. Shafik et al. [34] presented a hybrid inception-xception using a convolution NN for efficient plant disease classification and detection. Chen, Yang, and Sheng, [9] studied the numerical analysis of linearly implicit Euler method for age-structured SIS model. Rafique et al. [29] formulated the hybridized finite difference numerical method for obtaining the numerical solutions of the delayed fractional diabetes mellitus model. Avazzadeh et al. [4] presented an optimization method using generalized Laguerre polynomials and Lagrange multipliers to study a fractional tuberculosis model. Priyanga, Pattankar, and Sridevi [28] proposed a hybrid model using a recurrent NN and logistic chaos-based whale optimization for heart disease prediction from electronic health records. Iqbal et al. [16] presented the reciprocal domain adaptation network to the various issues of chronic kidney disease diagnosis. Amit Prakash [2] used the fractional Adams-Bashforth approach to examine the childhood disease. Dhar and Gupta [11] proposed a multi-step differential transformation method for solving tumor-immune model with B cells and monoclonal antibody drug. Avazzadeh et al. [5] presented an optimized method based on generalized Lerch polynomials to solve the

fractional-order model of CAR T-cell therapy for T-cell leukemia. Az-Zobi et al. [6] used the modified physics informed NNs with impacts of fractional derivative to obtain numerical solutions of modified Atangana Baleanu Caputo fractional advection dispersion models. Az-Zobi et al. [7] applied a feed-forward NN with five fully connected layers trained on data samples generated from the exact solutions of specific ordinary differential equations. Ruttanaprommarin et al. [31] applied a stochastic framework based on Levenberg–Marquardt backpropagation NNs for the Holling third kind of functional response delay differential model.

The current work introduces a new methodology to approximate the optimal solutions of susceptible human population $S(t)$ due to dental caries, the exposed bot not yet infected human population, $E(t)$, infected human population $I(t)$, and the recovered human population through the treatment $R(t)$ functions at time t, $t \in [0, T]$ using a neural network-based optimization (NNO) method and new fractional Narayana polynomials (FNPs). The mathematical model for simulating the spread of dental caries having the ordinary differential equation is given by [19]

$$\begin{cases} \frac{dS(t)}{dt} = \Lambda + \gamma R(t) - \left(\mu + \frac{\beta I(t)}{1+aI(t)}\right) S(t), \\ \frac{dE(t)}{dt} = \frac{\beta S(t) I(t)}{1+aI(t)} - (m+\rho)\, E(t), \\ \frac{dI(t)}{dt} = \rho E(t) - \left(\mu + \xi + \omega + \frac{\nu}{1+\eta I(t)}\right) I(t), \\ \frac{dR(t)}{dt} = \left(\omega + \frac{\nu}{1+\eta I(t)}\right) I(t) - (\mu+\gamma)\, R(t), \\ S(0) = S_0 \geq 0, \quad E(0) = E_0 \geq 0, \quad I(0) = I_0 \geq 0, \quad R(0) = R_0 \geq 0. \end{cases} \tag{1}$$

A description of the parameters in model (1) is provided in Table 1. The primary objectives of this research are as follows:

(i) This study is the first to present the concept of FNPs, a generalization of Narayana polynomials (NPs).

(ii) The convergence analysis, existence and uniqueness of solutions are provided for the method.

(iii) An optimization algorithm is derived using the Lagrange multiplier method.

(iv) A few terms of the FNPs are utilized to attain highly accurate results.

(v) The considered problem is transformed into a system of algebraic equations, which can be solved using an appropriate numerical method.

(vi) The proposed approach is computer-based and easy to apply in any language that supports programming.

(vii) The accuracy of the method is shown by solving numerical examples.

The paper is organized as follows: We present a description of NPs in Section 2. Section 3 presents a brief overview of the FNPs. Section 4 discusses the application of the suggested

Table 1: Definition of parameters in model (1) [19].

Parameter	Description
Λ	rate of recruitment of the population
γ	rate at which for recovered individuals move back to susceptible class
μ	natural death rate
β	the coefficient of dental infection transmission
a	the parameter that measures the inhibitory effects
m	mortality rate of the population and cut across all the compartments
ρ	rate at which exposed individuals became infected
ξ	death rate due to the infection
ω	recovery rate of infected individuals due to the response
ν	maximum medical resources supplied per unit time
η	A saturated factor that tracks the impact of delayed therapy on infected humans

NNO method to the given model. Sections 5 and 6 provide a convergence analysis of the method and existence and uniqueness of solutions for the system (1), respectively. To verify the theoretical results, Section 7 presents simulation results and applied examples. These simulations demonstrate the influence of various parameters on the model. Section 8 outlines the main conclusions of the paper and discusses their implications for future work.

2 NPs and function approximation

In this part of the paper, we discuss the definitions of NPs and the concept of function approximation using NPs.

Definition 1. Narayana numbers $\mathcal{N}_{i,j}$ are defined by the relations [26, 1]:

$$\mathcal{N}_{0,j} = \mathcal{N}_{j,0} = \delta_{j0} \quad (j \in \mathbb{N}_0), \qquad \mathcal{N}_{i,j} = \frac{1}{i}\binom{i}{j}\binom{i}{j-1} \quad (i, j \in \mathbb{N}),$$

where δ_{ij} denotes the Kronecker delta function.

Definition 2. The analytical form of the NPs, $\mathbb{A}_n(t)$, is obtained by [26, 1]

$$\mathbb{A}_n(t) = \sum_{k=0}^{n} \mathcal{N}_{n+1,k+1} t^k = \sum_{k=0}^{n} \frac{1}{n+1}\binom{n+1}{k+1}\binom{n+1}{k} t^k, \qquad n \in \mathbb{N}_0.$$

The first NPs are given by $\mathbb{A}_0(t) = 1$, $\mathbb{A}_1(t) = 1+t$, $\mathbb{A}_2(t) = 1+3t+t^2$, $\mathbb{A}_3(t) = 1+6t+6t^2+t^3$, and $\mathbb{A}_4(t) = 1+10t+20t^2+10t^3+t^4$.
A function $f(t)$ can be approximated using the first $(n+1)$ terms of the NPs as follows:

$$f(t) \simeq Q_n^T R_n S_n(t),$$

where $Q_n^T = [q_0 \;\; q_1 \;\; \dots \;\; q_n]$, and

$$R_n = \begin{pmatrix} 1 & 0 & \cdots & 0 \\ r_{1,0} & r_{1,1} & \cdots & r_{1,n} \\ \vdots & \vdots & \ddots & \vdots \\ r_{n,0} & r_{n,1} & \cdots & r_{n,n} \end{pmatrix}, \quad S_n(t) = [1 \;\; t \;\; t^2 \;\; \dots \;\; t^n]^T,$$

and

$$r_{ij} = \begin{cases} \dfrac{1}{i+1}\binom{i+1}{j+1}\binom{i+1}{j}, & i \geq j, \\ 0, & i < j. \end{cases}$$

3 FNPs and NN method

The definition of FNPs, their use in function approximation, and the Fractional Narayana polynomials neural network (FNPNN) model are introduced in this section.

Definition 3. The FNPs, $\mathbf{A}_m(t)$, are defined by the change of variable t^k into $t^{k+\alpha_k}$, $(k+\alpha_k > 0)$ on NPs as follows:

$$\mathbf{A}_m(t) = \sum_{k=0}^{m} \frac{1}{m+1}\binom{m+1}{k+1}\binom{m+1}{k} t^{k+\alpha_k}, \qquad m \in \mathbb{N}_0,$$

where α_k denotes a control parameter. When $\alpha_k = 0$, FNPs and classical NPs coincide.

3.1 Function approximations

A matrix representation of the functions $S(t)$, $E(t)$, $I(t)$ and $R(t)$ in (1) is provided below:

$$S(t) \simeq \mathbf{B}^T \mathbf{U} \mathbf{W}_{m_1}(t), \qquad E(t) \simeq \mathbf{C}^T \mathbf{V} \mathbf{W}_{m_2}(t),$$
$$I(t) \simeq \mathbf{D}^T \mathbf{P} \mathbf{W}_{m_3}(t), \qquad R(t) \simeq \mathbf{L}^T \mathbf{Q} \mathbf{W}_{m_4}(t),$$

where

$$\begin{aligned} \mathbf{B}^T &= [b_0 \;\; b_1 \dots b_{m_1}], \quad \mathbf{C}^T = [c_0 \;\; c_1 \dots c_{m_2}], \\ \mathbf{D}^T &= [d_0 \;\; d_1 \dots d_{m_3}], \quad \mathbf{L}^T = [l_0 \;\; l_1 \dots l_{m_4}], \end{aligned} \tag{2}$$

$$\mathbf{U} = \begin{pmatrix} 1 & 0 & 0 & \cdots & 0 \\ u_{1,0} & u_{1,1} & u_{1,2} & \cdots & u_{1,m_1} \\ \vdots & \vdots & \vdots & \cdots & \vdots \\ u_{m_1,0} & u_{m_1,1} & u_{m_1,2} & \cdots & u_{m_1,m_1} \end{pmatrix},$$
$$\mathbf{V} = \begin{pmatrix} 1 & 0 & 0 & \cdots & 0 \\ v_{1,0} & v_{1,1} & v_{1,2} & \cdots & v_{1,m_2} \\ \vdots & \vdots & \vdots & \cdots & \vdots \\ v_{m_2,0} & v_{m_2,1} & v_{m_2,2} & \cdots & v_{m_2,m_2} \end{pmatrix}, \tag{3}$$

$$\mathbf{P} = \begin{pmatrix} 1 & 0 & 0 & \cdots & 0 \\ p_{1,0} & p_{1,1} & p_{1,2} & \cdots & p_{1,m_3} \\ \vdots & \vdots & \vdots & \cdots & \vdots \\ p_{m_3,0} & p_{m_3,1} & p_{m_3,2} & \cdots & p_{m_3,m_3} \end{pmatrix},$$
$$\mathbf{Q} = \begin{pmatrix} 1 & 0 & 0 & \cdots & 0 \\ q_{1,0} & q_{1,1} & q_{1,2} & \cdots & q_{1,m_4} \\ \vdots & \vdots & \vdots & \cdots & \vdots \\ q_{m_4,0} & q_{m_4,1} & q_{m_4,2} & \cdots & q_{m_4,m_4} \end{pmatrix}, \tag{4}$$

$$u_{ij} = \begin{cases} \dfrac{1}{i+1}\binom{i+1}{j+1}\binom{i+1}{j}, & i \geq j, \\ 0, & i < j. \end{cases} \qquad i = 1, 2, \dots, m_1, \;\; j = 0, 1, \dots, m_1,$$

$$v_{ij} = \begin{cases} \dfrac{1}{i+1}\binom{i+1}{j+1}\binom{i+1}{j}, & i \geq j, \\ 0, & i < j. \end{cases} \qquad i = 1, 2, \ldots, m_2, \quad j = 0, 1, \ldots, m_2,$$

$$p_{ij} = \begin{cases} \dfrac{1}{i+1}\binom{i+1}{j+1}\binom{i+1}{j}, & i \geq j, \\ 0, & i < j. \end{cases} \qquad i = 1, 2, \ldots, m_3, \quad j = 0, 1, \ldots, m_3,$$

$$q_{ij} = \begin{cases} \dfrac{1}{i+1}\binom{i+1}{j+1}\binom{i+1}{j}, & i \geq j, \\ 0, & i < j. \end{cases} \qquad i = 1, 2, \ldots, m_4, \quad j = 0, 1, \ldots, m_4,$$

and

$$\mathbf{W}_{m_i}(t) \triangleq [w_0^i(t) \;\; w_1^i(t) \ldots w_{m_i}^i(t)]^T, \qquad i = 1, 2, 3, 4,$$

$$w_j^i(t) = \begin{cases} 1, & j = 0, \\ t^{j+\zeta_j^i}, & j = 1, 2, \ldots, m_i, \end{cases} \qquad i = 1, 2, 3, 4, \tag{5}$$

with ζ_j^i representing the control parameters as follows:

$$\mathfrak{Q}^1 = [\zeta_1^1 \;\; \zeta_2^1 \ldots \zeta_{m_1}^1], \quad \mathfrak{Q}^2 = [\zeta_1^{21} \;\; \zeta_2^2 \ldots \zeta_{m_2}^2],$$
$$\mathfrak{Q}^3 = [\zeta_1^3 \;\; \zeta_2^3 \ldots \zeta_{m_3}^3], \quad \mathfrak{Q}^4 = [\zeta_1^4 \;\; \zeta_2^4 \ldots \zeta_{m_4}^4].$$

A description of parameters in this section is provided in Table 2.

3.2 FNPNN

NNs are known as effective machine learning algorithms that are ideal for solving complicated problems [39, 38, 40]. In order to efficiently and accurately solve a mathematical model of dental caries infection, a novel FNPNN method is proposed in this paper. The FNPNN method is structured with three layers that function as described below:

(i) The input t is provided by the network's input layer.

Table 2: Definition of parameters in Section 3.

Parameter	Description
t	Time
$\mathbb{A}_n(t)$	NPs
$\mathbf{A}_m(t)$	FNPs
$\mathbf{B}$, $\mathbf{C}$, $\mathbf{D}$, $\mathbf{L}$	Vectors of free coefficients
ζ_j^i	Control parameters
$\mathbf{W}_{m_1}$, $\mathbf{W}_{m_2}$, $\mathbf{W}_{m_3}$, $\mathbf{W}_{m_4}$	Vectors of control parameters
$\mathbf{U}$, $\mathbf{V}$, $\mathbf{P}$, $\mathbf{Q}$	Matrices of NP coefficients
$\mathfrak{Q}^i(t)$	Vectors of FNPs
$\tilde{\mathbf{S}}(t)$, $\tilde{\mathbf{E}}(t)$, $\tilde{\mathbf{I}}(t)$, $\tilde{\mathbf{R}}(t)$	Approximations of $\mathbf{S}(t)$, $\mathbf{E}(t)$, $\mathbf{I}(t)$ and $\mathbf{R}(t)$

(ii) In the network's hidden layer, we select FNPs of varying degrees as activation functions.
(iii) The network's output layer is constructed as a weighted linear combination of FNPs. Figure 1 illustrates the NN structure utilized in this study. Note that the activation function is the function that acts upon the input to get the output of the network. There are many types of activation functions such as the sigmoid function, the hyperbolic tangent function, the ReLu function and others [8]. In this context, the inverse hyperbolic sine (arcsine) functions are used as activation functions. Consequently, the following are the results of the FNPNN, using input data t and parameters $\mathbf{B}$, $\mathbf{C}$, $\mathbf{D}$ and $\mathbf{L}$:

$$\begin{aligned} \mathbf{S}(t,\mathbf{B}) &= arc\sinh(S(t)), \qquad \mathbf{E}(t,\mathbf{C}) = arc\sinh(E(t)), \\ \mathbf{I}(t,\mathbf{D}) &= arc\sinh(I(t)), \qquad \mathbf{R}(t,\mathbf{L}) = arc\sinh(R(t)), \end{aligned} \tag{6}$$

where $S(t)$, $E(t)$, $I(t)$ and $R(t)$ are linear combinations expressed as follows:

$$\begin{aligned} S(t) &= \sum_{i=0}^{m_1} b_i \mathbf{A}_i(t), \qquad E(t) = \sum_{j=0}^{m_2} c_j \mathbf{A}_j(t), \\ I(t) &= \sum_{k=0}^{m_3} d_k \mathbf{A}_k(t), \qquad R(t) = \sum_{p=0}^{m_4} l_k \mathbf{A}_p(t), \end{aligned}$$

and $\mathbf{B}$, $\mathbf{C}$, $\mathbf{D}$ and $\mathbf{L}$ vectors are given by

$$\mathbf{B}^T = [b_0 \;\; b_1 \ldots b_{m_1}], \qquad \mathbf{C}^T = [c_0 \;\; c_1 \ldots c_{m_2}],$$

$$\mathbf{D}^T = [d_0 \;\; d_1 \dots d_{m_3}], \qquad \mathbf{L}^T = [l_0 \;\; l_1 \dots l_{m_4}].$$

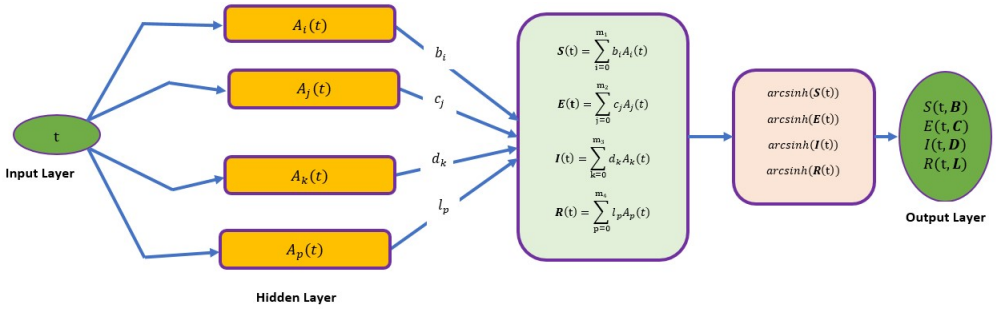


Figure 1: FNPNN architecture.

4 Description of the approach

The focus of this section is to introduce the FNPNN approach for solving the dental caries infection model in (1). We approximate $S(t)$, $E(t)$, $I(t)$ and $R(t)$ by using the activation functions as

$$\begin{aligned} S(t) &\simeq \tilde{S}(t) = S_0 + t\mathbf{S}(t, \mathbf{B}), & E(t) &\simeq \tilde{E}(t) = E_0 + t\mathbf{E}(t, \mathbf{C}), \\ I(t) &\simeq \tilde{I}(t) = I_0 + t\mathbf{I}(t, \mathbf{D}), & R(t) &\simeq \tilde{R}(t) = R_0 + t\mathbf{R}(t, \mathbf{L}). \end{aligned} \tag{7}$$

We know that $S(t)$, $E(t)$, $I(t)$ and $R(t)$ satisfy the initial conditions. By applying (7) to the initial conditions of problem (1), we derive the following properties:

$$\begin{aligned} \Delta_1 &\triangleq \tilde{S}(0) - S_0 \simeq 0, & \Delta_2 &\triangleq \tilde{E}(0) - E_0 \simeq 0, \\ \Delta_3 &\triangleq \tilde{I}(0) - I_0 \simeq 0, & \Delta_4 &\triangleq \tilde{R}(0) - R_0 \simeq 0. \end{aligned} \tag{8}$$

Using the approximations of (7) in (1), we have

$$\begin{cases} \frac{d\tilde{S}(t)}{dt} - \Lambda - \gamma\tilde{R}(t) + \left(\mu + \frac{\beta\tilde{I}(t)}{1+a\tilde{I}(t)}\right)\tilde{S}(t) \triangleq \mathscr{R}_1(t, \mathbf{B}, \mathbf{W}^1), \\ \frac{d\tilde{E}(t)}{dt} - \frac{\beta\tilde{S}(t)\tilde{I}(t)}{1+a\tilde{I}(t)} + (m+\rho)\,\tilde{E}(t) \triangleq \mathscr{R}_2(t, \mathbf{C}, \mathbf{W}^2), \\ \frac{d\tilde{I}(t)}{dt} - \rho\tilde{E}(t) + \left(\mu + \xi + \omega + \frac{\nu}{1+\eta\tilde{I}(t)}\right)\tilde{I}(t) \triangleq \mathscr{R}_3(t, \mathbf{D}, \mathbf{W}^3), \\ \frac{d\tilde{R}(t)}{dt} - \left(\omega + \frac{\nu}{1+\eta\tilde{I}(t)}\right)\tilde{I}(t) + (\mu+\gamma)\,\tilde{R}(t) \triangleq \mathscr{R}_4(t, \mathbf{L}, \mathbf{W}^4). \end{cases} \tag{9}$$

Here, $\mathbf{B}$, $\mathbf{C}$, $\mathbf{D}$ and $\mathbf{L}$ denote unknown free coefficients. Additionally, $\mathbf{W}^i$, $(i = 1, 2, 3, 4)$, are unknown control parameters, which are defined as follows:

$$\mathbf{W}^i = \left[\zeta_1^i \;\; \zeta_2^i \;\; \ldots \;\; \zeta_{m_i}^i\right], \qquad i = 1, 2, 3, 4.$$

The 2-norm of the residual functions is given by

$$\begin{aligned} &\mathfrak{R}\left(\mathbf{B}, \mathbf{C}, \mathbf{D}, \mathbf{L}, \mathbf{W}^1, \mathbf{W}^2, \mathbf{W}^3, \mathbf{W}^4\right) \\ &= \int_0^T \left(\mathscr{R}_1^2(t, \mathbf{B}, \mathbf{W}^1) + \mathscr{R}_2^2(t, \mathbf{C}, \mathbf{W}^2) + \mathscr{R}_3^2(t, \mathbf{D}, \mathbf{W}^3) + \mathscr{R}_4^2(t, \mathbf{L}, \mathbf{W}^4)\right) dt. \end{aligned} \tag{10}$$

It is required to evaluate the unknown vectors $\mathbf{B}$, $\mathbf{C}$, $\mathbf{D}$, $\mathbf{L}$, $\mathbf{W}^1$, $\mathbf{W}^2$, $\mathbf{W}^3$, and $\mathbf{W}^4$ by employing the optimization problem as follows:

$$\min\, \mathfrak{R}\left(\mathbf{B}, \mathbf{C}, \mathbf{D}, \mathbf{L}, \mathbf{W}^1, \mathbf{W}^2, \mathbf{W}^3, \mathbf{W}^4\right), \tag{11}$$

under the conditions in (8) where $\mathfrak{R}$ is the objective function. To address this optimization problem, we assume the following condition:

$$\begin{aligned} &\mathcal{J}^*[\mathbf{B}, \mathbf{C}, \mathbf{D}, \mathbf{L}, \mathbf{W}^1, \mathbf{W}^2, \mathbf{W}^3, \mathbf{W}^4, \theta] \\ &= \mathfrak{R}\left(\mathbf{B}, \mathbf{C}, \mathbf{D}, \mathbf{L}, \mathbf{W}^1, \mathbf{W}^2, \mathbf{W}^3, \mathbf{W}^4\right) + \theta\,\Delta. \end{aligned} \tag{12}$$

Note that θ is the Lagrange multipliers vector. By utilizing the Lagrange multiplier technique, we can derive the necessary and sufficient conditions for optimality, which are as follows:

$$\begin{cases} \dfrac{\partial\mathcal{J}^*}{\partial\theta} = 0, & \dfrac{\partial\mathcal{J}^*}{\partial\mathbf{B}} = 0, & \dfrac{\partial\mathcal{J}^*}{\partial\mathbf{C}} = 0, \\ \dfrac{\partial\mathcal{J}^*}{\partial\mathbf{D}} = 0, & \dfrac{\partial\mathcal{J}^*}{\partial\mathbf{L}} = 0, & \dfrac{\partial\mathcal{J}^*}{\partial\mathbf{W}^i} = 0, \qquad i = 1, 2, 3, 4. \end{cases} \tag{13}$$

By solving that system for the unknown vectors $\mathbf{B}$, $\mathbf{C}$, $\mathbf{D}$, $\mathbf{L}$, $\mathbf{W}^1$, $\mathbf{W}^2$, $\mathbf{W}^3$, and $\mathbf{W}^4$, we attain the approximate optimal solution for (1). In this study, the nonlinear algebraic system

given in (13) is solved using the 'fsolve' tool in Maple 2024. The procedure above outlines the application of the FNPNN method to solve the dental caries infection model presented in (1). The step-by-step algorithm and flowchart of the explained approach are concisely stated below:

FNPNN Algorithm for solving a mathematical model of the dental caries infection in (1)

Input: Initial conditions, Number of basis functions (m_i, $i = 1, 2, 3, 4$).

* Determine the unknown vectors $\mathbf{B}$, $\mathbf{C}$, $\mathbf{D}$, $\mathbf{L}$ and matrices of NPs coefficients $\mathbf{U}$, $\mathbf{V}$, $\mathbf{P}$ and $\mathbf{Q}$ based on (2)–(4).
* Determine the basis functions $w_j^i(t)$ by (5).
* Determine the activation functions $\mathbf{S}(t, \mathbf{B})$, $\mathbf{E}(t, \mathbf{C})$, $\mathbf{I}(t, \mathbf{D})$ and $\mathbf{R}(t, \mathbf{L})$ using (6).
* Calculate:
  - The initial conditions Δ_i for $i = 1, 2, 3, 4$ using (8).
  - The residual functions $\mathscr{R}_i$ for $i = 1, 2, 3, 4$ using (9).
  - The 2-norm of the residual functions $\mathfrak{R}\left(\mathbf{B}, \mathbf{C}, \mathbf{D}, \mathbf{L}, \mathbf{W}^1, \mathbf{W}^2, \mathbf{W}^3, \mathbf{W}^4\right)$ using (10).
* Minimize the objective function $\mathfrak{R}\left(\mathbf{B}, \mathbf{C}, \mathbf{D}, \mathbf{L}, \mathbf{W}^1, \mathbf{W}^2, \mathbf{W}^3, \mathbf{W}^4\right)$ under the constraints defined in (11).
* Apply the Lagrange multiplier technique $\mathcal{J}^*[\mathbf{B}, \mathbf{C}, \mathbf{D}, \mathbf{L}, \mathbf{W}^1, \mathbf{W}^2, \mathbf{W}^3, \mathbf{W}^4, \theta]$ using (12).
* Solve the nonlinear algebraic system using (13).

Output: The approximate solutions are $S(t) \simeq \tilde{S}(t) = S_0 + t\mathbf{S}(t, \mathbf{B})$, $E(t) \simeq \tilde{E}(t) = E_0 + t\mathbf{E}(t, \mathbf{C})$, $I(t) \simeq \tilde{I}(t) = I_0 + t\mathbf{I}(t, \mathbf{D})$, $R(t) \simeq \tilde{R}(t) = R_0 + t\mathbf{R}(t, \mathbf{L})$.

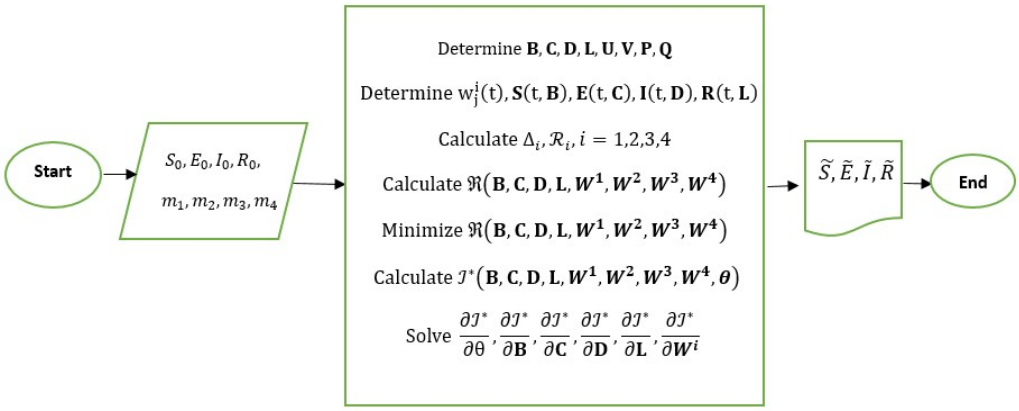


Figure 2: The flowchart of the explained approach.

5 Convergence analysis

In this section, we provide theorems that guarantee the convergence of the proposed method.

Theorem 1. Consider (e_n) is a sequence in X such that $Span\{\mathrm{e}_n | n \in \mathbb{N}\}$ is dense in X; $(X, \|\cdot\|)$ is a normed linear space; and $x_0 \in X$. Let (x_n) be the best approximation to x_0 in the $Span\{\mathrm{e}_1, \ldots, \mathrm{e}_n\}$; then (x_n) converges to x_0.

Proof. Since the closure of $Span\{e_n | n \in \mathbb{N}\}$ is equal to X, there exists a sequence (y_k) in $Span\{e_n | n \in \mathbb{N}\}$ with $y_k \to x_0$. We suppose that $y_k \in Span\{e_1, \ldots, e_{n_k}\}$, in which (n_k) is a monotonically increasing sequence in $\mathbb{N}$, without losing generality. Therefore, we can write

$$\|x_{n_k} - x_0\| \leq \|y_k - x_0\| \to 0, \quad (\text{as } k \to \infty). \tag{14}$$

It is also evident that the sequence $(\|x_n - x_0\|)_{n\in\mathbb{N}}$, consisting of non-negative real numbers is non-increasing. By applying (14), this sequence contains a convergent subsequence. As a result, (x_n) converges to x_0. □

Theorem 2. Let $g : [0, 1] \to \mathbb{R}$ be a continuous function. Then, for every $t \in (0, 1)$ and $\epsilon > 0$, there exists an FNPs, $\mathbf{A}_m(t)$, such that

$$|g(t) - \mathbf{A}_m(t)| < \epsilon.$$

Proof. Let $\epsilon > 0$ be arbitrarily chosen. In view of the Weierstrass theorem [20], there exists a polynomial $P_m(t) = a_0 + a_1 t + a_2 t^2 + \cdots + a_m t^m$, $t \in (0, 1)$, such that

$$\sup_{t\in(0,1)} |g(t) - P_m(t)| < \frac{\epsilon}{2}.$$

We construct a FNPs, $\mathbf{A}_m(t)$, as follows:

Let $t \in (0, 1)$. We consider a sequence $\{\gamma_{k,n}\}_{n\in\mathbb{N}}$ of real numbers such that $\rho_{k,n} \to \frac{-\ln\left(\binom{m}{k}(1-t)^{m-k}\right)}{\ln(t)}$ as $n \to \infty$, for all $k = 0, 1, 2, 3, \ldots, m$, where $\binom{m}{k} = \frac{m!}{k!(m-k)!}$. This ensures that $t^{\rho_{k,n}} \to \frac{1}{c_{mk}}$ as $n \to \infty$, for all $k = 0, 1, 2, 3, \ldots, m$, where

$$c_{mk} = \frac{-\ln\left(\binom{m}{k}(1-t)^{m-k}\right)}{\ln(t)}.$$

Hence, for every $\epsilon > 0$, there exist $N_0, N_1, \ldots, N_m$ in $\mathbb{N}$ such that

$$|1 - c_{mk} t^{\rho_{k,n}}| < \frac{\epsilon}{2\max\{|a_0|, |a_1|, \ldots, |a_m|\}(m+1)}, \quad \forall\ k = 0, 1, 2, 3, \ldots, m.$$

Setting $N = \max\{N_0, N_1, \ldots, N_m\}$ and

$$\mathbf{A}_m(t) = a_0 c_{m0} t^{\rho_{0,N}} + a_1 c_{m1} t^{1+\rho_{1,N}} + a_2 c_{m2} t^{2+\rho_{2,N}} + \cdots + a_m c_{mm} t^{m+\rho_{m,N}},$$

we conclude that

$$|P_m(t) - \mathbf{A}_m(t)| < \frac{\epsilon}{2}.$$

This implies that

$$|g(t) - \mathbf{A}_m(t)| \leq |g(t) - P_m(t)| + |P_m(t) - \mathbf{A}_m(t)| < \frac{\epsilon}{2} + \frac{\epsilon}{2} = \epsilon.$$

□

Remark 1. For each $T > 0$, we consider $X = L^2[0, T]$, equipped with $\|\cdot\|_2$, and $\mathrm{e}_n := \mathbf{A}_n$, the FNPs. Then, by Theorem 1, it follows that for every $x_0 \in L^2[0, T]$ the sequence (x_n) of best approximation of x_0 in $Span\{\mathbf{A}_1, \ldots, \mathbf{A}_n\}$, converges (in $\|\cdot\|_2$) to x_0.

Remark 2. Let $\tilde{S}(t)$, $\tilde{E}(t)$, $\tilde{I}(t)$ and $\tilde{R}(t)$ be the FNPNN approximate solutions of $S(t)$, $E(t)$, $I(t)$ and $R(t)$, respectively. We refer the readers to [30] for the error bound of approximations.

6 Existence and uniqueness of solutions for the system (1)

Lemma 1. [21, 23] Let $\Omega \subseteq \mathbb{R}^n$, and consider the differential system

$$\dot{x}(t) = f(t, x), \quad (t > 0),$$

with initial condition x_0, where $f : [0, \infty) \times \Omega \to \mathbb{R}^n$ satisfies a local Lipschitz condition with respect to x on $[0, \infty) \times \Omega$. Then this equation admits a unique solution $x(t)$.

Theorem 3. For $0 < t < \infty$, the system of differential equations (1) has a unique solution $\big(S(t), E(t), I(t), R(t)\big)$.

Proof. Let $F : [0, \infty) \times \mathbb{R}^4 \to \mathbb{R}^4$ be defined for each $t \in [0, \infty)$, $a \neq 0$, $1 + aI(t) > 0$, $1 + \eta I(t) > 0$ and $X = (S, E, I, R) \in \mathbb{R}^4$ by $F(t, X) = F(t, S, E, I, R) = \big(f_1(X), f_2(X), f_3(X), f_4(X)\big)$, where

$$\begin{aligned}
f_1(X) &= \Lambda + \gamma R(t) - \left(\mu + \tfrac{\beta I(t)}{1+aI(t)}\right) S(t), \\
f_2(X) &= \tfrac{\beta S(t) I(t)}{1+aI(t)} - (m + \rho)\, E(t), \\
f_3(X) &= \rho E(t) - \left(\mu + \xi + \omega + \tfrac{\nu}{1+\eta I(t)}\right) I(t), \\
f_4(X) &= \left(\omega + \tfrac{\nu}{1+\eta I(t)}\right) I(t) - (\mu + \gamma)\, R(t).
\end{aligned} \tag{15}$$

In order to prove the uniqueness of the solution for system (1), it suffices, according to Lemma 1, to demonstrate that F is locally Lipschitz in the region $[0,T]\times\mathcal{B}$, where M and T are both arbitrary positive real numbers and $\mathcal{B}:=\{X\in\mathbb{R}^4:\ \|X\|_\infty\leq M\}$. Now, let $X=(S,E,I,R),\tilde{X}=(\tilde{S},\tilde{E},\tilde{I},\tilde{R})\in\mathcal{B}$. Then, it follows that

$$
\begin{aligned}
&\|F(X)-F(\tilde{X})\|_1\\
&=\left|f_1(X)-f_1(\tilde{X})\right|+\left|f_2(X)-f_2(\tilde{X})\right|+\left|f_3(X)-f_3(\tilde{X})\right|+\left|f_4(X)-f_4(\tilde{X})\right|\\
&=\Bigg|\Lambda+\gamma R(t)-\left(\mu+\frac{\beta I(t)}{1+aI(t)}\right)S(t)-\\
&\quad\left(\Lambda+\gamma\tilde{R}(t)-\left(\mu+\frac{\beta\tilde{I}(t)}{1+a\tilde{I}(t)}\right)\tilde{S}(t)\right)\Bigg|\\
&\quad+\left|\frac{\beta S(t)I(t)}{1+aI(t)}-(m+\rho)\,E(t)-\left(\frac{\beta\tilde{S}(t)\tilde{I}(t)}{1+a\tilde{I}(t)}-(m+\rho)\,\tilde{E}(t)\right)\right|\\
&\quad+\left|\rho E(t)-\left(\mu+\xi+\omega+\frac{\nu}{1+\eta I(t)}\right)I(t)\right.\\
&\quad\left.-\left(\rho\tilde{E}(t)-\left(\mu+\xi+\omega+\frac{\nu}{1+\eta\tilde{I}(t)}\right)\tilde{I}(t)\right)\right|\\
&\quad+\left|\left(\omega+\frac{\nu}{1+\eta I(t)}\right)I(t)-(\mu+\gamma)\,R(t)\right.\\
&\quad\left.-\left(\left(\omega+\frac{\nu}{1+\eta\tilde{I}(t)}\right)\tilde{I}(t)-(\mu+\gamma)\,\tilde{R}(t)\right)\right|\\
&\leq|\gamma|\left|R(t)-\tilde{R}(t)\right|+\left(|\mu|+\left|\frac{\beta}{a}\right|\right)\left|S(t)-\tilde{S}(t)\right|\\
&\quad+\left|\frac{\beta}{a}\right|\left|S(t)-\tilde{S}(t)\right|+(|m|+|\rho|)\left|E(t)-\tilde{E}(t)\right|\\
&\quad+|\rho|\left|E(t)-\tilde{E}(t)\right|+(|\mu|+|\xi|+|\omega|)\left|I(t)-\tilde{I}(t)\right|\\
&\quad+|\omega|\left|I(t)-\tilde{I}(t)\right|+(|\mu|+|\gamma|)\left|R(t)-\tilde{R}(t)\right|\\
&=\Big(|\mu|+2|\gamma|\Big)\left|R(t)-\tilde{R}(t)\right|+\left(|\mu|+2\left|\frac{\beta}{a}\right|\right)\left|S(t)-\tilde{S}(t)\right|\\
&\quad+\Big(|m|+2|\rho|\Big)\left|E(t)-\tilde{E}(t)\right|+\Big(|\mu|+|\xi|+2|\omega|\Big)\left|I(t)-\tilde{I}(t)\right|
\end{aligned}
$$

$$\leq \zeta\Big(\Big|R(t) - \tilde{R}(t)\Big| + \Big|S(t) - \tilde{S}(t)\Big| + \Big|E(t) - \tilde{E}(t)\Big| + \Big|I(t) - \tilde{I}(t)\Big| \Big)$$

$$= \zeta \left\|X - \tilde{X}\right\|_1,$$

where $\zeta = \max\left\{|\mu| + 2|\gamma|, \ \ |\mu| + 2\left|\frac{\beta}{a}\right|, \ \ |m| + 2|\rho|, \ \ |\mu| + |\xi| + 2|\omega|\right\}$. Thus F is locally Lipschitz and, therefore, by using Lemma 1 the dental caries infection model (1) admits a unique solution $\big(S(t), E(t), I(t), R(t)\big)$. □

Theorem 4. The solutions $S(t)$, $E(t)$, $I(t)$ and $R(t)$ of system (1) with initial values $S(0) = S_0 \geq 0$, $E(0) = E_0 \geq 0$, $I(0) = I_0 \geq 0$, $R(0) = R_0 \geq 0$ are positive for all $t > 0$.

Proof. The proof follows the same procedure as the one in Huo, Chen, and Wang [15]. □

6.1 Basic reproduction number

The basic reproduction number, R_0, is defined as the measure used to characterize the potential for an infectious organism to spread through a fully susceptible population, indicating the maximum potential rate of spread in that population. R_0 remains constant in the absence of prior immunity, while the effective reproduction number, R_t, decreases as immunity develops within the population. By employing the next-generation matrix technique [19], a basic reproduction number R_0 can be computed to obtain the rate of transmission of the model, which is given as

$$R_0 = \frac{\beta\rho\Lambda}{\mu(\mu+\rho)(\mu+\xi+\omega+\nu)}. \tag{16}$$

It stands for the typical quantity of secondary infections brought on by the original infection. We refer the reader to [19] for the basic reproduction number.

7 Solution method and approximate results

In this section, we validate and demonstrate the applicability of the proposed strategy for solving a mathematical model of the dental caries infection in (1). All the numerical calculations are performed using Maple 2024 and the CPU time (in seconds) is provided for an Intel Core i7 3.00 GHz personal computer with 8 GB RAM. As the analytical solution for the given problem is unknown, we verify the reliability and accuracy of the technique by analyzing the residual error function. In order to draw the figures of approximations obtained for $S(t)$, $E(t)$, $I(t)$ and $R(t)$,

the following initial values and parameter values are considered [19]:

$$S_0 = 3,\ \ E_0 = 1,\ \ I_0 = 3,\ \ R_0 = 0,\ \ \Lambda = 0.70,\ \ \gamma = 0.000001,\ \ \mu = 0.13,$$
$$\beta = 0.05,\ \ a = 0.0002,\ \ m = 0.0077,\ \ \rho = 0.8,\ \ \xi = 0.05,\ \ \omega = 0.5,$$
$$\nu = 0.5,\ \ \eta = 0.000001.$$

The results obtained are depicted in Figures 3–6 with $m_1 = m_2 = m_3 = m_4 = 2$ (left side) and $m_1 = m_3 = 2$, $m_2 = m_4 = 3$ (right side) over a time period of 1 month. The runtime (in seconds) for our suggested technique and the optimal values for the residual function with several m_1, m_2, m_3 and m_4 values are provided in Tables 3 and 4. The mathematical model of dental caries infection (1) is also solved using the techniques discussed in section 4, but with the Chebyshev polynomials neural network (CPNN). The behavior of the approximate solutions $S(t)$, $E(t)$, $I(t)$ and $R(t)$ with CPNN, $m_1 = m_2 = m_3 = m_4 = 2$ and $\beta = 0.07$ is shown in Figure 7. Table 4 lists the values obtained for the optimal residual function for various values of m_1, m_2, m_3 and m_4 using both CPNN and FNPNN over a time period of 1 month. The results presented in Figure 7 and Table 4 indicate that the proposed method is more accurate than the CPNN-based results.

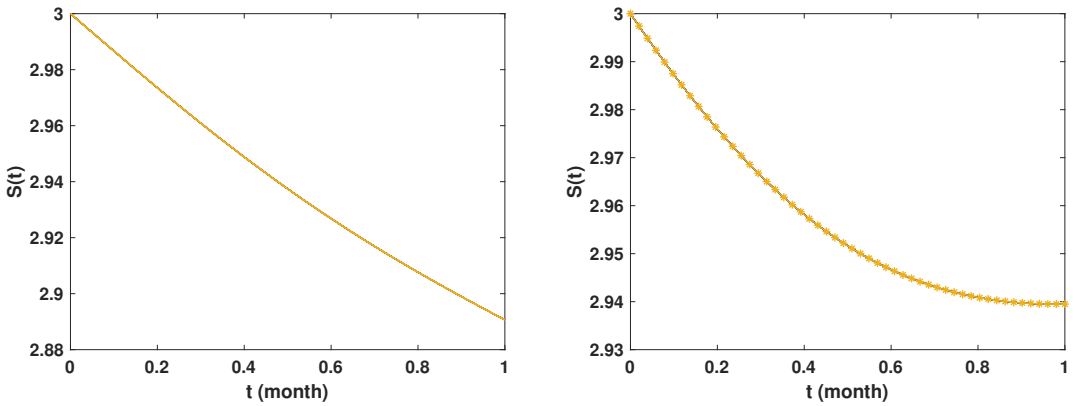


Figure 3: The FNPNN solutions of $S(t)$ with $m_1 = m_2 = m_3 = m_4 = 2$ (left side) and $m_1 = m_3 = 2$, $m_2 = m_4 = 3$ (right side).

Sensitivity analysis plays a central role in appraising the soundness and reliability of mathematical models across various disciplines. It helps distinguish which parameters have the most significant effect on outputs of the given model. By determining the sensitivity of the given model to different parameters, researchers can optimize the model structure or parameter values to achieve better performance. In this section, some scenarios will be designed to demonstrate

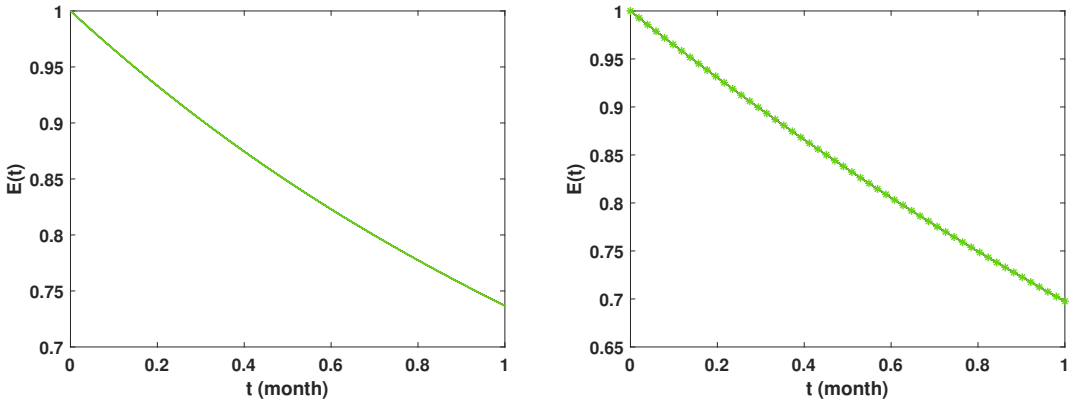


Figure 4: The FNPNN solutions of $E(t)$ with $m_1 = m_2 = m_3 = m_4 = 2$ (left side) and $m_1 = m_3 = 2$, $m_2 = m_4 = 3$ (right side).

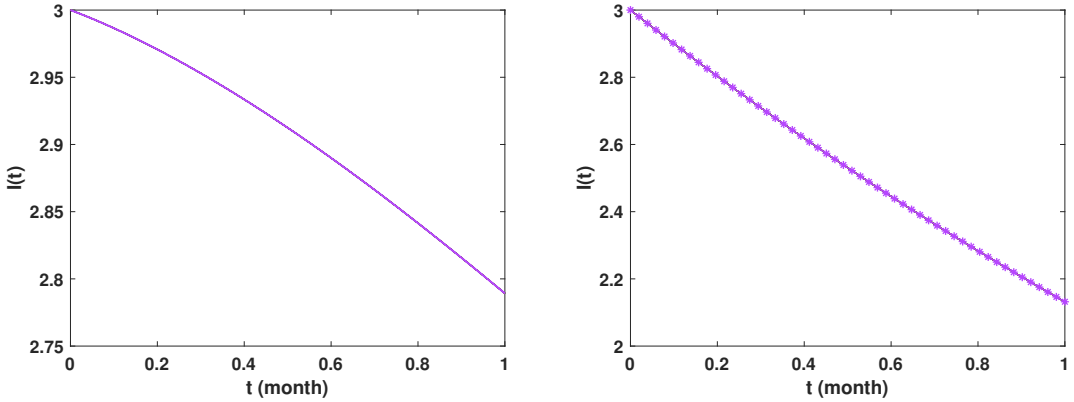


Figure 5: The FNPNN solutions of $I(t)$ with $m_1 = m_2 = m_3 = m_4 = 2$ (left side) and $m_1 = m_3 = 2$, $m_2 = m_4 = 3$ (right side).

Table 3: The runtime of the FNPNN method with several values of m_i, $i = 1, 2, 3, 4$.

case	m_1	m_2	m_3	m_4	CPU times
1	2	2	2	2	5.27
2	2	3	2	3	8.34
3	3	3	3	3	13.84

the sensitivity of the suggested model to diverse parameters.

1. Sensitivity to β: By choosing $\beta = 0.07$, model (1) is solved by the method stated in the previous subsection and figures of $S(t)$, $E(t)$, $I(t)$ and $R(t)$ are depicted in Figure 8 with $m_1 = m_2 = m_3 = m_4 = 2$ over a time period of 1 month.

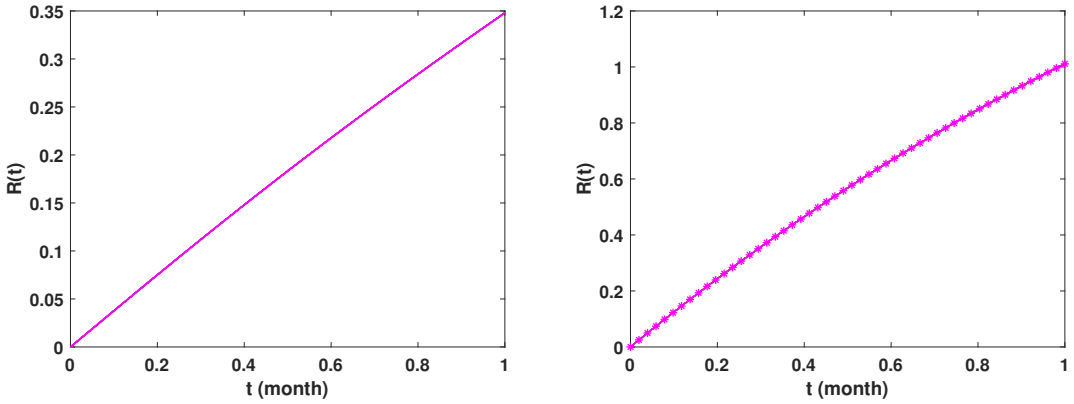


Figure 6: The FNPNN solutions of $R(t)$ with $m_1 = m_2 = m_3 = m_4 = 2$ (left side) and $m_1 = m_3 = 2$, $m_2 = m_4 = 3$ (right side).

Table 4: The optimal values of the residual function using CPNN and FNPNN with different values of m_i, where $i = 1, 2, 3, 4$.

case	m_1	m_2	m_3	m_4	Residual function (CPNN)	Residual function (FNPNN)
1	2	2	2	2	$5.8412E-03$	$2.0748E-07$
2	2	3	2	3	$2.8564E-04$	$3.2851E-08$
3	3	3	3	3	$9.5681E-05$	$3.7066E-10$

2. Sensitivity to Λ: By choosing values of Λ as $\Lambda = 0.40$, model (1) is solved by the method stated in the previous subsection and figures of $S(t)$, $E(t)$, $I(t)$ and $R(t)$ are depicted in Figure 9 with $m_1 = m_2 = m_3 = m_4 = 2$ over a time period of 1 month.

The number of susceptible human population $S(t)$ due to dental caries, the exposed human population but not infected $E(t)$ yet and the infected human population $I(t)$ decrease over time (Figures 3–5). The number of recovered human population through the treatment $R(t)$ increases (Figure 6). After applying the sensitivity analysis to β and Λ, we observe changes in Figures 8 and 9, indicating that model (1) is sensitive to these parameters.

Remark 3. For sensitivity analysis of the method, we refer the reader to [13].

8 Concluding remarks

This study introduces a novel algorithm, FNPNN, designed to enhance the efficiency of optimization processes in solving the dental caries infection model. This study employs the optimization approach to demonstrate the feasibility of approximating the solution to the dental caries in-

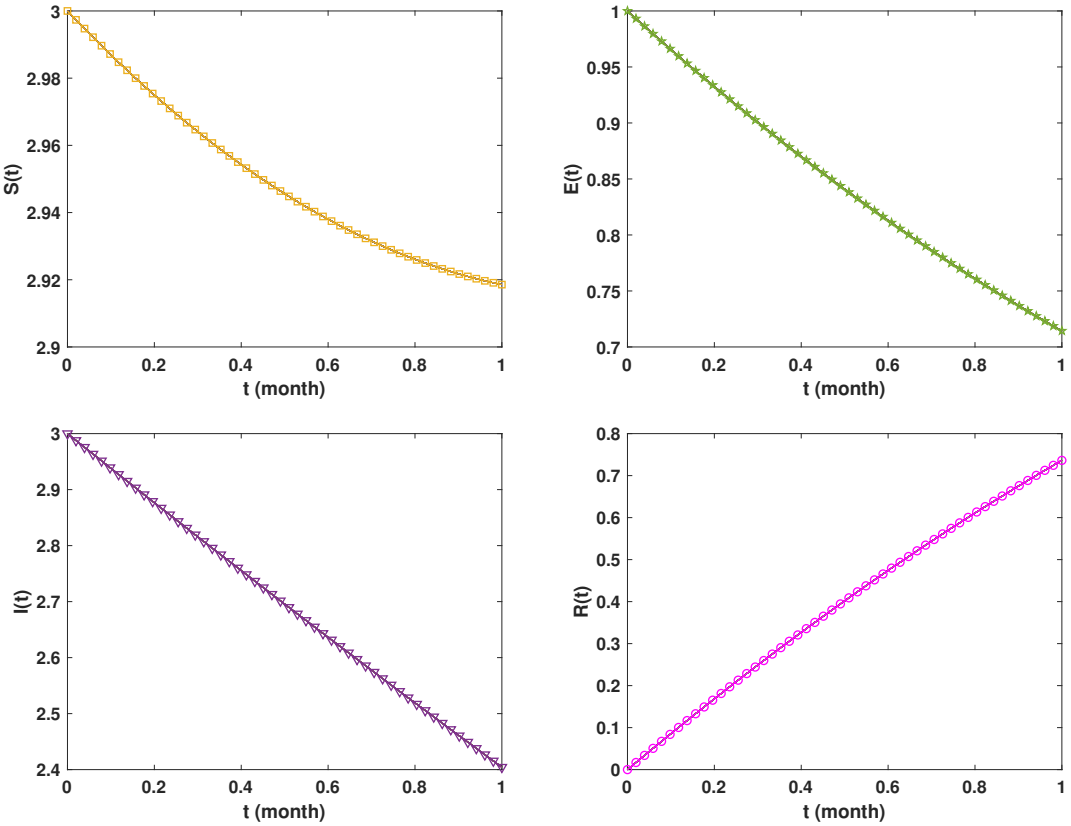


Figure 7: The CPNN solutions of $S(t)$, $E(t)$, $I(t)$ and $R(t)$ with $m_1 = m_2 = m_3 = m_4 = 2$ and $\beta = 0.07$.

fection model using an NN. The combination of the optimization method and NN refinement provides a promising framework for enhancing the precision and effectiveness of solving systems of differential equations in scientific and engineering applications. Tables 3 and 4 and Figures 3–9 show that the proposed model solution is reliable and produces the approximate solution with a minimal number of basis functions. In conclusion, numerical experiments are provided to deepen the understanding of the approach and to illustrate the detailed procedure for solving the dental caries infection model, thereby making the concepts clearer and more comprehensible.

Future research directions

The process of FNPNN by using the optimization method can be used to solve the fractional variable-order models, fractional optimal control problems, fractional-order partial differential

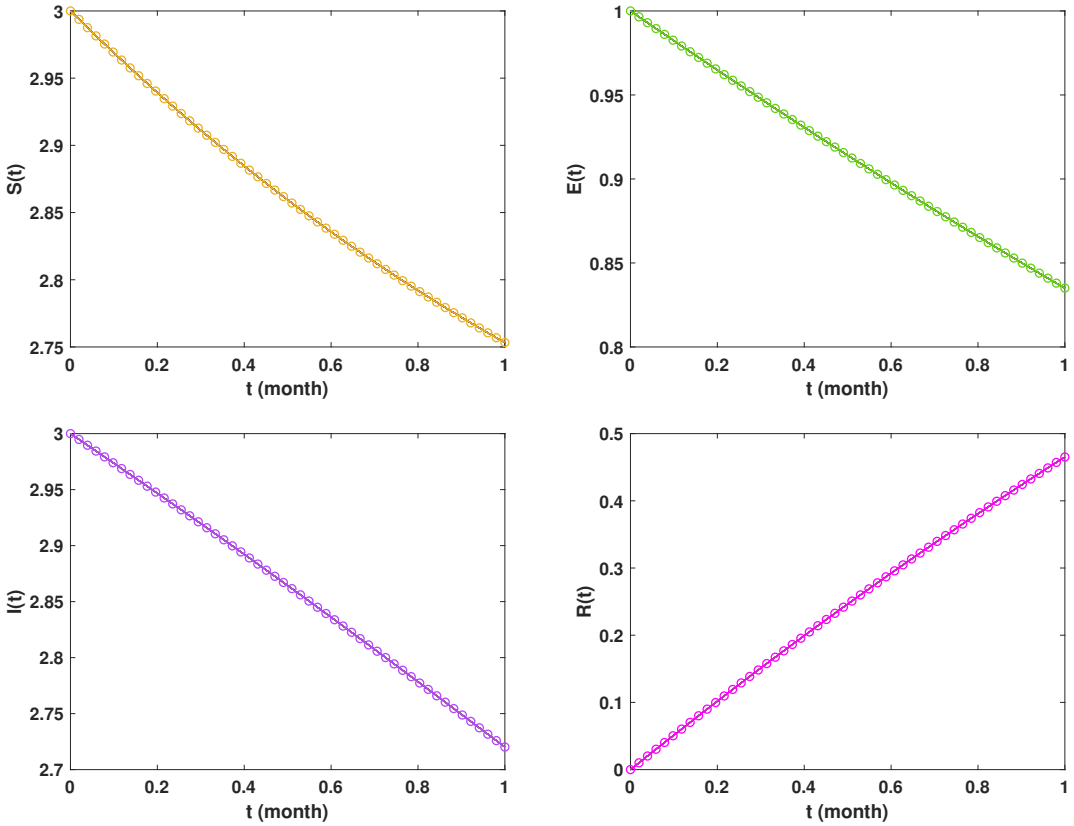


Figure 8: The FNPNN solutions of $S(t)$, $E(t)$, $I(t)$ and $R(t)$ with $m_1 = m_2 = m_3 = m_4 = 2$ and $\beta = 0.07$.

equations, fractional-order systems of partial differential equations, and various models in bioscience, etc.

Funding

This research received no external funding.

Conflicts of Interest

The authors declare no conflicts of interest.

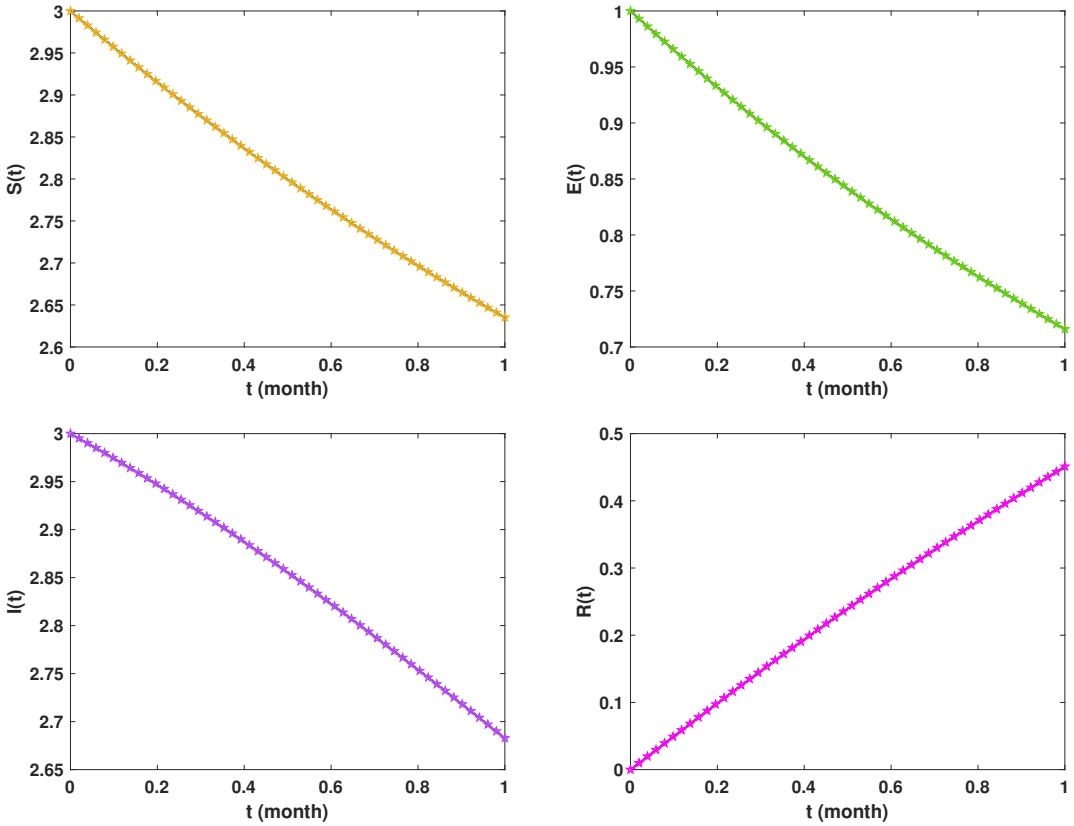


Figure 9: The FNPNN solutions of $S(t)$, $E(t)$, $I(t)$ and $R(t)$ with $m_1 = m_2 = m_3 = m_4 = 2$ and $\Lambda = 0.40$.

References

[1] Agapito, J., Mestre, A., Petrullo, P. and Torres, M.M., *Combinatorics of a generalized Narayana identity,* Linear Algebra Appl. 503 (2016) 56–82.

[2] Amit Prakash, R., *Numerical simulation of SIR childhood diseases model with fractional Adams–Bashforth method,* Math. Methods Appl. Sci. 46(12) (2023) 12340–12360.

[3] Anusha Bamini, A.M., Chitra, R., Brindha, D. and Chenthil Jegan, T.M. *A novel approach for premature detection of Alzheimer's disease using convolutional neural network in deep learning technique,* Wireless Pers. Commun. 135 (2024) 639–654.

[4] Avazzadeh, Z., Hassani, H., Agarwal, P., Mehrabi, S., Ebadi, M.J. and Dahaghin, M.S., *An optimization method for studying fractional-order tuberculosis disease model via generalized Laguerre polynomials,* Soft Comput. 27 (2023) 9519–9531.

[5] Avazzadeh, Z., Hassani, H., Ebadi, M.J., Zarei-Behjani, Z., Bayati Eshkaftaki, A., Mehrabi, S. and Haghighat, S., *Generalized Lerch polynomials: application in fractional model of CAR-T cells for T-cell leukemia,* Eur. Phys. J. Plus. 138(12) (2023) 1–13.

[6] Az-Zobi, E.A., Hussain, A.S., Iqbal, M., Aljohani, A., Tashtoush, M.A., Alsubaie, N.E., Al-Hamarneh, F.K.A., Nazar, N.M. and Baleanu, D., *Analytical and numerical solutions of MABC fractional advection dispersion models by utilizing the modified physics informed neural networks with impacts of fractional derivative,* Sci. Rep. 15 (2025) 43366.

[7] Az-Zobi, E.A., Shah, R., Alyousef, H.A., Tiofack, C.G.L. and El-Tantawy, S.A., *On the feed-forward neural network for analyzing pantograph equations,* AIP Adv. 14(2) (2024) 025042.

[8] Calin, O., *Deep learning architectures,* Springer, 2020.

[9] Chen, Z., Yang, Z. and Sheng, D., *Numerical analysis of linearly implicit Euler method for age-structured SIS model,* J. Appl. Math. Comput. 70 (2024) 969–996.

[10] Dawes, C. and Wong, D.T., *Role of saliva and salivary diagnostics in the advancement of oral health,* J. Dent. Res. 98(2) (2019) 133–141.

[11] Dhar, B. and Kumar Gupta, P., *A numerical approach of tumor-immune model with B cells and monoclonal antibody drug by multi-step differential transformation method,* Math. Methods Appl. Sci. 44(5) (2021) 4058–4070.

[12] Featherstone, J.D.B., *The caries balance: Contributing factors and early detection,* J. Calif. Dent. Assoc. 31(2) (2003) 129–133.

[13] Guo, Y., Ma, B. and Wu, R., *On sensitivity analysis of parameters for fractional differential equations with Caputo derivatives,* Electron. J. Qual. Theory Differ. Equ. 118 (2016) 1–17.

[14] He, J., *A new high-precision numerical method for solving the HIV infection model of CD4(+) cells*, Physica A. 653 (2024) 130090.

[15] Huo, H.F., Chen, R. and Wang, X.Y., *Modelling and stability of HIV/AIDS epidemic model with treatment,* Appl. Math. Modell. 40(13-14) (2016) 6550–6559.

[16] Iqbal, S., Qureshi, A.N., Alhussein, M., Aurangzeb, K., Zubair, M. and Hussain, A., *A novel reciprocal domain adaptation neural network for enhanced diagnosis of chronic kidney disease,* Expert Syst. 42(2) (2025) e13825.

[17] Kassebaum, N.J., Bernabe, E., Dahiya, M., Bhandari, B., Murray, C.J.L. and Marcenes, W., *Global burden of untreated caries: A systematic review and metaregression,* J. Dent. Res. 94(5) (2015) 650–658.

[18] Kassebaum, N.J., Smith, A.G.C., Bernabe, E., Fleming, T.D., Reynolds, A.E., Vos, T., Murray, C.J.L. and Marcenes, W., *Collaborators global, regional, and national prevalence, incidence, and disability-adjusted life years for oral conditions for 195 Countries, 1990-2015: A systematic analysis for the global burden of diseases, injuries, and risk factors,* J. Dent. Res. 96(4) (2017) 380–387.

[19] Khirsariya, S.R. and Chauhan, J.P., *Numerical and theoretical insights into fractional dental caries infection model,* Iran J. Sci. 49 (2025) 1605–1618.

[20] Kreyszig, E., *Introductory functional analysis with applications,* John Wiley and Sons. Inc. 1978.

[21] Li, Y. Chen, Y. and Podlubny, I., *Stability of fractional-order non linear dynamic systems: Lyapunov direct method and generalized Mittag-Leffler stability,* Comput. Math. Appl. 59(10) (2010) 1810–1821.

[22] Li, M. and Yang, Z., *Numerical analysis of an age-structured model for HIV viral dynamics with latently infected T cells based on collocation methods,* Math. Comput. Simul. 230 (2025) 289–305.

[23] Maji, C., Mukherjee, D. and Kesh, D., *Study of a fractional-order model of chronic wasting disease,* Math. Methods Appl. Sci. 43(7) (2020) 4669–4682.

[24] Mortazavi, S., Enshaei, Z. and Farajzadegan, Z., *Development of caries risk assessment tool for Iranian preschoolers: A primary validation study,* Int. J. Prev. Med. (2017) PMID :29184643.

[25] Peres, M.A., Macpherson, L.M.D., Weyant, R.J., Daly, B., Venturelli, R., Mathur, M.R., Listl, S., Celeste, R.K., Guarnizo-Herreno, C.C., Kearns, C., Benzian, H., Allison, P. and Watt, R.G., *Oral diseases: A global public health challenge,* Lancet. 394(10194) (2019) 249–260.

[26] Petkovic, M.D., Barry, P. and Rajkovic, P., *Closed-form expression for Hankel determinants of the Narayana polynomials,* Czech. Math. J. 62(1) (2012) 39–57.

[27] Pitts, N.B., Zero, D.T., Marsh, P.D., Ekstrand, K., Weintraub, J.A., Ramos-Gomez, F., Tagami, J., Twetman, S., Tsakos, G. and Ismail, A., *Dental caries,* Nat. Rev. Dis. Primers. 3 (2017) 17030.

[28] Priyanga, P., Pattankar, V.V. and Sridevi, S., *A hybrid recurrent neural network-logistic chaos-based whale optimization framework for heart disease prediction with electronic health records,* Comput. Intell. 37(1) (2021) 315–343.

[29] Rafique, M., Ur Rehamn, M.A., Rafiq, M., Iqbal, Z., Ahmed, N., Alhazmi, H., Niazai, S. and Khan, I., *Time delayed fractional diabetes mellitus model and consistent numerical algorithm,* Sci. Rep. 14 (2024) 23871.

[30] Rahimkhani, P. and Ordokhani, Y., *Orthonormal Bernoulli wavelets neural network method and its application in astrophysics,* Comput. Appl. Math. 40 (2021) 78.

[31] Ruttanaprommarin, N., Sabir, Z., Sandoval Nunez, R.A., Az-Zobi, E.A., Weera, W., Botmart, T. and Zamart, C., *A stochastic framework for solving the prey-predator delay differential model of Holling type-III,* Comput. Mater. Continua. 74(3) (2023) 5915–5930.

[32] Sabir, Z., Athar Mehmood, M., Umar, M., Salahshour, S., Altun, Y., Arbi, A. and Ali, M.R., *A numerical treatment through Bayesian regularization neural network for the chickenpox disease model,* Comput. Biol. Med. 187 (2025) 109807.

[33] Sabir, Z., Ben Said, S. and Al-Mdallal, Q., *A fractional order numerical study for the influenza disease mathematical model,* Alexandria Engineering Journal, 65 (2023) 615–626.

[34] Shafik, W., Tufail, A., Silva, C.L.D. and Haji Mohd Apong, R.A.A., *A novel hybrid inception-xception convolutional neural network for efficient plant disease classification and detection,* Sci. Rep. 15 (2025) 3936.

[35] Sheiham, A., *Dietary effects on dental diseases,* Public Health Nutr. 4(2B) (2001) 569–591.

[36] Sheiham, A. and James, W.P.T., *A new understanding of the relationship between sugars, dental caries and fluoride use: implications for limits on sugars consumption,* Public Health Nutr. 17(10) (2014) 2176–2184.

[37] Slobodnikova, L., Halasa, A.I., Kalmanova, S., Calkovsky, B., Juricek, R., Malachovsky, I., Repiska, V., Skerenova, M. and Janickov, M., *Genetic factors influencing susceptibility to dental caries*, Bratisl. Med. J. 125 (2024) 635–647.

[38] Verma, A. and Kumar, M., *Numerical solution of Bagley-Torvik equations using Legendre artificial neural network method,* Evol. Intell. 14 (2021) 2027–2037.

[39] Verma, A. and Kumar, M. *Numerical solution of third-order Emden–Fowler type equations using artificial neural network technique,* Eur. Phys. J. Plus. 135(9) (2020) 751.

[40] Verma, A., Sumelka, W. and Yadav, P.K. *The numerical solution of nonlinear fractional Lienard and Duffing equations using orthogonal perceptron,* Symmetry, 15(9) (2023) 1753.

[41] Wang, X., Willing, M.C., Marazita, M.L., Wendell, S., Warren, J.J., Broffitt, B., Smith, B., Busch, T., Lidral, A.C. and Levy, S.M., *Genetic and environmental factors associated with dental caries in children: The Iowa Fluoride Study,* Caries Res. 46(3) (2012) 177–184.

[42] Wang, Z., Yang, Z., Yang, G. and Zhang, C., *Numerical analysis of age-structured HIV model with general transmission mechanism,* Commun. Nonlinear Sci. Numer. Simul. 134 (2024) 108020.

[43] Wang, X., Zhang. P., Lu, H., Luo, D., Yang, D., Li, K., Qiu, S., Zeng, H. and Zeng, X., *Risk prediction models for dental caries in children and adolescents: a systematic review and meta-analysis,* BMJ Open. 15(3) (2025) e088253.